

A Parametric Finite Element For Simulating Solid-State Dewetting Problems

Quan Zhao

with Prof. Weizhu Bao, Dr. Wei Jiang and Dr. Yan Wang

Department of Mathematics
National University of Singapore

June 3, 2016

- Mathematical model for weakly anisotropic surface energies
- Variational formulation and parametric finite element method
- Simulation results
- Extension to the strongly anisotropic case
- Summary

Mathematical Model

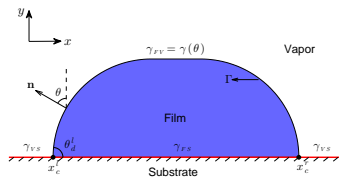


Figure: A schematic illustration of a solid thin film on a flat, rigid substrate

Mathematical Model

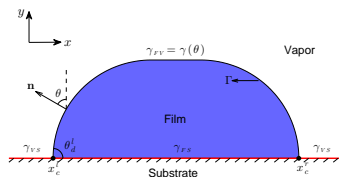


Figure: A schematic illustration of a solid thin film on a flat, rigid substrate

♠ *Sharp Interface Model* – Dynamics Y. Wang *et al.* 2015

$$\begin{aligned}\partial_t \vec{X} &= \partial_{ss} \mu \vec{n}, & 0 < s < L(t), & & t > 0, \\ \mu &= [\gamma(\theta) + \gamma''(\theta)] \kappa, & \kappa &= -(\partial_{ss} \vec{X}) \cdot \vec{n};\end{aligned}$$

Weak Anisotropy $\gamma(\theta) + \gamma''(\theta) > 0 \quad \forall \theta \in [-\pi, \pi]$, $\vec{X} = (x(s, t), y(s, t))$.

Mathematical Model

With following boundary conditions:

(i) *Contact point condition*

$$y(0, t) = 0, \quad y(L, t) = 0, \quad t \geq 0,$$

(ii) *Relaxed contact angle condition*

$$\frac{dx_c^l}{dt} = \eta f(\theta_d^l; \sigma), \quad \frac{dx_c^r}{dt} = -\eta f(\theta_d^r; \sigma), \quad t \geq 0,$$

(iii) *Zero-mass flux condition*

$$\partial_s \mu(0, t) = 0, \quad \partial_s \mu(L, t) = 0, \quad t \geq 0;$$

where $\theta_d^l := \theta_d^l(t)$ and $\theta_d^r := \theta_d^r(t)$ are the (dynamic) contact angles at the left and right contact points, respectively, $0 < \eta < \infty$ denotes the contact line mobility, and $f(\theta; \sigma)$ (*anisotropic young's equation*) is defined as:

$$f(\theta; \sigma) = \gamma(\theta) \cos \theta - \gamma'(\theta) \sin \theta - \sigma, \quad \theta \in [-\pi, \pi],$$

High order and *nonlinear* geometric equations with boundary conditions

♠ "Marker-particle" method (explicit finite-difference scheme) [Wong *et al.* 2000](#); [Y. Wang *et al.* 2015](#)

1. First update the inner mesh points by the explicit finite difference scheme
2. renew the two contact points according to the contact angle condition.
3. Do polynomial interpolation and redistribute the mesh points uniformly with respect to arc length.

High order and *nonlinear* geometric equations with boundary conditions

- ♠ "Marker-particle" method (explicit finite-difference scheme) [Wong et al. 2000](#); [Y. Wang et al. 2015](#)
 1. First update the inner mesh points by the explicit finite difference scheme
 2. renew the two contact points according to the contact angle condition.
 3. Do polynomial interpolation and redistribute the mesh points uniformly with respect to arc length.
- ♠ Parametric finite element method for surface diffusion flow([E.Bansch et al., 2004](#); [J.W. Barrett et al., 2007](#))

Variational Formulation

- Introduce a new time-independent *spatial variable* $\rho \in I := [0, 1]$ to parameterize the curve $\Gamma(t)$

$$\Gamma(t) = \vec{X}(\rho, t) : I \times [0, T] \rightarrow \mathbb{R}^2.$$

- Define the following inner product for any scalar (or vector) functions.

$$\langle u, v \rangle_{\Gamma} := \int_{\Gamma(t)} u(s)v(s) ds = \int_I u(s(\rho, t))v(s(\rho, t))|\partial_{\rho}\vec{X}| d\rho, \forall u, v \in L^2(I),$$

- Define the functional space for the solution of the solid-state dewetting problem as

$$H_{a,b}^1(I) = \{u \in H^1(I) : u(0) = a, u(1) = b\},$$

- Rewrite the governing equations as

$$\begin{aligned}\partial_t \vec{X} \cdot \vec{n} &= \partial_{ss} \mu, \\ \mu &= [\gamma(\theta) + \gamma'(\theta)] \kappa, \\ \kappa \vec{n} &= -\partial_{ss} \vec{X};\end{aligned}$$

Variational Formulation

Given an initial curve $\Gamma(0) = \vec{X}(\rho, 0) = \vec{X}_0(s)$, then for any time $t \in (0, T]$, find $\Gamma(t) = \vec{X}(\rho, t) \in H_{a,b}^1(I) \times H_0^1(I)$ with the x -coordinate positions of moving contact points $a = x_c^l(t) \leq x_c^r(t) = b$, $\mu(\rho, t) \in H^1(I)$, and $\kappa(\rho, t) \in H^1(I)$ such that

$$\langle \partial_t \vec{X}, \varphi \vec{n} \rangle_\Gamma + \langle \partial_s \mu, \partial_s \varphi \rangle_\Gamma = 0, \quad \forall \varphi \in H^1(I),$$

$$\langle \mu, \psi \rangle_\Gamma - \langle [\gamma(\theta) + \gamma''(\theta)] \kappa, \psi \rangle_\Gamma = 0, \quad \forall \psi \in H^1(I),$$

$$\langle \kappa \vec{n}, \vec{\omega} \rangle_\Gamma - \langle \partial_s \vec{X}, \partial_s \vec{\omega} \rangle_\Gamma = 0, \quad \forall \vec{\omega} \in H_0^1(I) \times H_0^1(I),$$

Proposition (Mass conservation)

Assume that $(\vec{X}(\rho, t), \mu(\rho, t), \kappa(\rho, t))$ be a weak solution of the variational problem, then the total mass of the thin film is conserved during the evolution, i.e.,

$$A(t) \equiv A(0) = \int_{\Gamma(0)} y_0(s) \partial_s x_0(s) ds, \quad t \geq 0.$$

Proposition (Energy dissipation)

Assume that $(\vec{X}(\rho, t), \mu(\rho, t), \kappa(\rho, t))$ be a weak solution of the variational problem and it has higher regularity, i.e.,

$\vec{X}(\rho, t) \in C^1(C^2(I); [0, T]) \times C^1(C^2(I); [0, T])$, then the total energy of the thin film is decreasing during the evolution, i.e.,

$$W(t) \leq W(t_1) \leq W(0) = \int_{\Gamma(0)} \gamma(\theta) ds - (x_c^r(0) - x_c^l(0))\sigma, \quad t \geq t_1 \geq 0.$$

Parametric Finite Element Method

- Divide $I = \bigcup_{j=1}^N I_j = \bigcup_{j=1}^N [\rho_{j-1}, \rho_j]$ with $h = 1/N$ and $\rho_j = jh$, take time steps as $0 = t_0 < t_1 < t_2 < \dots$ with $\tau_m := t_{m+1} - t_m$ for $m \geq 0$.
- Define the space

$$V^h := \{u \in C(I) : u|_{I_j} \in P_1, \quad j = 1, 2, \dots, N\} \subset H^1(I),$$
$$\mathcal{V}_{a,b}^h := \{u \in V^h : u(0) = a, u(1) = b\} \subset H_{a,b}^1(I),$$

- Define the mass lumped inner product $\langle \cdot, \cdot \rangle_{\Gamma^m}^h$ over $\Gamma^m = \vec{X}^m$ as

$$\langle u, v \rangle_{\Gamma^m}^h := \frac{1}{2} \sum_{j=1}^N \left| \vec{X}^m(\rho_j) - \vec{X}^m(\rho_{j-1}) \right| \left[(u \cdot v)(\rho_j^-) + (u \cdot v)(\rho_{j-1}^+) \right],$$

where $u(\rho_j^\pm) = \lim_{\rho \rightarrow \rho_j^\pm} u(\rho)$.

♠ **A semi-implicit *parametric finite element method* (PFEM)**

For $m \geq 0$, first update the two contact point positions $x_c^l(t_{m+1})$ and $x_c^r(t_{m+1})$ via the relaxed contact angle condition by using the forward Euler method and then find $\Gamma^{m+1} = \vec{X}^{m+1} \in \mathcal{Y}_{a,b}^h \times \mathcal{Y}_0^h$ with $a := x_c^l(t_{m+1}) \leq b := x_c^r(t_{m+1})$, $\mu^{m+1} \in V^h$ and $\kappa^{m+1} \in V^h$ such that

$$\begin{aligned} \left\langle \frac{\vec{X}^{m+1} - \vec{X}^m}{\tau_m}, \varphi_h \vec{n}^m \right\rangle_{\Gamma^m}^h + \langle \partial_s \mu^{m+1}, \partial_s \varphi_h \rangle_{\Gamma^m}^h &= 0, \quad \forall \varphi_h \in V^h, \\ \langle \mu^{m+1}, \psi_h \rangle_{\Gamma^m}^h - \langle [\gamma(\theta^m) + \gamma''(\theta^m)] \kappa^{m+1}, \psi_h \rangle_{\Gamma^m}^h &= 0, \quad \forall \psi_h \in V^h, \\ \langle \kappa^{m+1} \vec{n}^m, \vec{\omega}_h \rangle_{\Gamma^m}^h - \langle \partial_s \vec{X}^{m+1}, \partial_s \vec{\omega}_h \rangle_{\Gamma^m}^h &= 0, \quad \forall \vec{\omega}_h \in \mathcal{Y}_0^h \times \mathcal{Y}_0^h. \end{aligned}$$

Numerical Results

♠ Convergence order test ($\gamma = 1$)

$$e_{h,\tau}(t) = \|\vec{X}_{h,\tau} - \vec{X}_{\frac{h}{2},\frac{\tau}{4}}\|_{L^\infty} = \max_{0 \leq j \leq N} \min_{\rho \in [0,1]} |\vec{X}_{h,\tau}(\rho_j, t) - \vec{X}_{\frac{h}{2},\frac{\tau}{4}}(\rho, t)|,$$

Table: The numerical convergence orders in the L^∞ norm sense for a *closed curve* evolution under the *isotropic* surface diffusion flow.

$e_{h,\tau}(t)$	$h = h_0$ $\tau = \tau_0$	$h_0/2$ $\tau_0/2^2$	$h_0/2^2$ $\tau_0/2^4$	$h_0/2^3$ $\tau_0/2^6$	$h_0/2^4$ $\tau_0/2^8$
$e_{h,\tau}(t = 0.5)$	4.58E-3	1.09E-3	2.63E-4	6.40E-5	1.58E-5
order	–	2.07	2.05	2.04	2.02
$e_{h,\tau}(t = 2.0)$	3.61E-3	9.43E-4	2.45E-4	6.31E-5	1.61E-5
order	–	1.94	1.95	1.96	1.97
$e_{h,\tau}(t = 5.0)$	3.63E-3	9.47E-4	2.46E-4	6.33E-5	1.62E-5
order	–	1.94	1.95	1.96	1.97

Numerical Results

♠ Convergence order test ($\gamma = 1 + \beta \cos(k(\theta + \varphi))$)

Table: The numerical convergence orders in the L^∞ norm sense for a *closed curve* evolution under the *anisotropic* surface diffusion flow, where the parameters of the surface energy are chosen as: $k = 4, \beta = 0.06, \varphi = 0$.

$e_{h,\tau}(t)$	$h = h_0$	$h_0/2$	$h_0/2^2$	$h_0/2^3$	$h_0/2^4$
	$\tau = \tau_0$	$\tau_0/2^2$	$\tau_0/2^4$	$\tau_0/2^6$	$\tau_0/2^8$
$e_{h,\tau}(t = 0.5)$	3.82E-2	1.43E-2	6.05E-3	2.19E-3	6.76E-4
order	—	1.41	1.24	1.47	1.69
$e_{h,\tau}(t = 2.0)$	1.80E-2	6.48E-3	2.47E-3	7.99E-4	2.24E-4
order	—	1.47	1.39	1.63	1.83
$e_{h,\tau}(t = 5.0)$	1.74E-2	6.19E-3	2.36E-3	7.60E-4	2.12E-4
order	—	1.49	1.39	1.64	1.84

Numerical Results

♠ Convergence order test ($\gamma = 1 + \beta \cos(k(\theta + \varphi))$)

Table: The numerical convergence orders in the L^∞ norm sense for an *open curve* evolution under the *anisotropic* surface diffusion flow (solid-state dewetting with anisotropic surface energies), where the computational parameters are chosen as: $k = 4, \beta = 0.06, \varphi = 0, \sigma = \cos(5\pi/6)$.

$e_{h,\tau}(t)$	$h = h_0$ $\tau = \tau_0$	$h_0/2$ $\tau_0/2^2$	$h_0/2^2$ $\tau_0/2^4$	$h_0/2^3$ $\tau_0/2^6$
$e_{h,\tau}(t = 0.5)$	3.91E-2	1.73E-2	7.52E-3	3.40E-3
order	–	1.17	1.20	1.16
$e_{h,\tau}(t = 2.0)$	3.58E-2	1.73E-2	7.71E-3	3.46E-3
order	–	1.05	1.17	1.15
$e_{h,\tau}(t = 5.0)$	2.75E-2	1.39E-2	6.61E-3	3.10E-3
order	–	0.98	1.07	1.09

Numerical Results

- Several steps in the evolution of small islands and $\gamma(\theta) = 1 + \beta \cos(k(\theta + \varphi))$

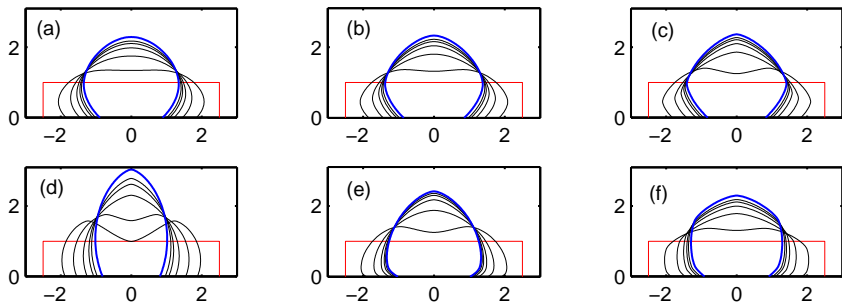


Figure: $\varphi = 0$, $\sigma = \cos(3\pi/4)$ in all cases. Figures (a)-(c) are results for $\beta = 0.02, 0.04, 0.06$ ($k = 4$ is fixed), and Figures (d)-(f) are simulation results for (d) $k = 2, \beta = 0.32$, (e) $k = 3, \beta = 0.1$, and (f) $k = 6, \beta = 0.022$, respectively.

Numerical Results

- ♠ Mass conservation, energy dissipation and long time equidistribution

Define the mesh-distribution function as

$$\Psi(t = t_m) = \Psi^m := \frac{\max_{1 \leq j \leq N} \|\vec{X}^m(\rho_j) - \vec{X}^m(\rho_{j-1})\|}{\min_{1 \leq j \leq N} \|\vec{X}^m(\rho_j) - \vec{X}^m(\rho_{j-1})\|}$$

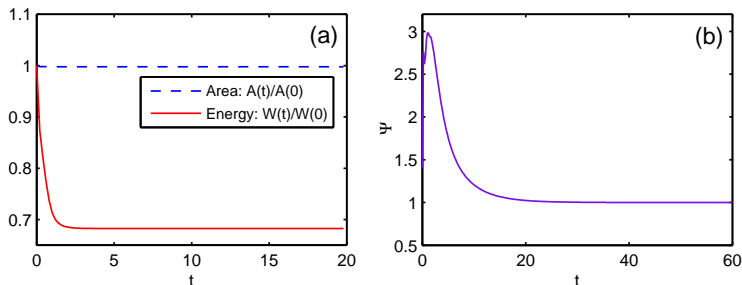
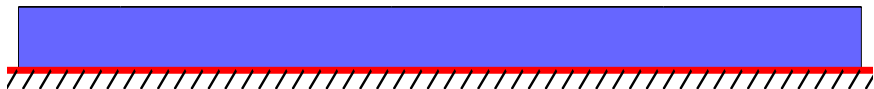


Figure: (a) The temporal evolution of the normalized total free energy and the normalized area (mass); (b) the temporal evolution of the mesh distribution $\Psi(t)$.

Numerical Results

♠ pinch off for large islands

$$L = 60, m = 4, \beta = 0.06, \sigma = \cos(5\pi/6)$$



Numerical Results

♠ Mass conservation and energy dissipation for large island

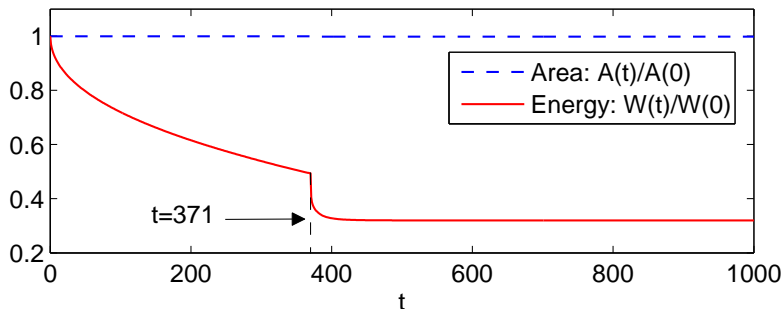


Figure: The corresponding temporal evolution for the normalized total free energy and the normalized area (mass).

- ♠ Mild restrictions on numerical stability ($\tau_m = ch^2$)
- ♠ Solving linear systems, very efficient to implement
- ♠ Allow a tangential movement of the mesh points and long time equidistribution. [J.W. Barrett et al., 2007](#)
- ♠ Maintain mass conservation and energy dissipation in the sense of weak formulation where mass $A(t)$ and energy $W(t)$ defined as

$$A(t) = \int_{\Gamma(t)} y \partial_s x \, ds, \quad W(t) = \int_{\Gamma(t)} \gamma(\theta) \, ds - (x_c^r - x_c^l) \sigma, \quad t \geq 0,$$

Extension to Strongly Anisotropic Case

♠ *Regularized sharp interface model* ($\gamma(\theta) + \gamma''(\theta) < 0$ for some θ)

the sharp-interface model will become mathematically ill-posed. The Willmore energy regularization will be added into the total interfacial energy as

$$W_\varepsilon := W + \frac{\varepsilon^2}{2} \int_\Gamma \kappa^2 ds = \int_\Gamma \gamma(\theta) ds + \frac{\varepsilon^2}{2} \int_\Gamma \kappa^2 ds - (x_c^r - x_c^l) \sigma,$$

So the regularized sharp interface model for strongly anisotropic surface energies ([W. Jiang et al. \(2015\)](#)) will be

$$\begin{aligned} \partial_t \vec{X} &= \partial_{ss} \mu \vec{n}, & 0 < s < L(t), & & t > 0, \\ \mu &= [\gamma(\theta) + \gamma''(\theta)] \kappa - \varepsilon^2 \left(\frac{\kappa^3}{2} + \partial_{ss} \kappa \right), & \kappa &= -(\partial_{ss} \vec{X}) \cdot \vec{n}; \end{aligned}$$

Boundary Conditions For Strong Case

With the following boundary conditions,

(i) *Contact point condition*

$$y(0, t) = 0, \quad y(L, t) = 0, \quad t \geq 0,$$

(ii) *Relaxed contact angle condition*

$$\frac{dx_c^l}{dt} = \eta f_\varepsilon(\theta_d^l; \sigma), \quad \frac{dx_c^r}{dt} = -\eta f_\varepsilon(\theta_d^r; \sigma), \quad t \geq 0,$$

(iii) *Zero-mass flux condition*

$$\partial_s \mu(0, t) = 0, \quad \partial_s \mu(L, t) = 0, \quad t \geq 0,$$

(iv) *Zero-curvature condition*

$$\kappa(0, t) = 0, \quad \kappa(L, t) = 0, \quad t \geq 0;$$

where $f_\varepsilon(\theta; \sigma) := \gamma(\theta) \cos \theta - \gamma'(\theta) \sin \theta - \sigma - \varepsilon^2 \partial_s \kappa \sin \theta$ for $\theta \in [-\pi, \pi]$, which reduces to $f(\theta; \sigma)$ when $\varepsilon \rightarrow 0^+$.

Parametric Finite Element Method

For $m \geq 0$, first update the two contact point positions $x_c^l(t_{m+1})$ and $x_c^r(t_{m+1})$ via the relaxed contact angle condition (0.1) by using the forward Euler method and then find $\Gamma^{m+1} = \vec{X}^{m+1} \in \mathcal{Y}_{a,b}^h \times \mathcal{Y}_0^h$ with the x-coordinate positions of the moving contact points $a := x_c^l(t_{m+1}) \leq b := x_c^r(t_{m+1})$, $\mu^{m+1} \in V^h$ and $\kappa^{m+1} \in \mathcal{Y}_0^h$ such that

$$\begin{aligned} \left\langle \frac{\vec{X}^{m+1} - \vec{X}^m}{\tau_m}, \varphi_h \vec{n}^m \right\rangle_{\Gamma^m}^h + \langle \partial_s \mu^{m+1}, \partial_s \varphi_h \rangle_{\Gamma^m}^h &= 0, \quad \forall \varphi_h \in V^h, \\ \langle \mu^{m+1}, \psi_h \rangle_{\Gamma^m}^h - \left\langle \left[\tilde{\gamma}(\theta^m) - \frac{\varepsilon^2}{2} (\kappa^m)^2 \right] \kappa^{m+1}, \psi_h \right\rangle_{\Gamma^m}^h \\ &\quad - \varepsilon^2 \langle \partial_s \kappa^{m+1}, \partial_s \psi_h \rangle_{\Gamma^m}^h = 0, \quad \forall \psi_h \in \mathcal{Y}_0^h, \\ \langle \kappa^{m+1} \vec{n}^m, \vec{\omega}_h \rangle_{\Gamma^m}^h - \langle \partial_s \vec{X}^{m+1}, \partial_s \vec{\omega}_h \rangle_{\Gamma^m}^h &= 0, \quad \forall \vec{\omega}_h \in \mathcal{Y}_0^h \times \mathcal{Y}_0^h, \end{aligned}$$

where $\tilde{\gamma}(\theta^m) = \gamma(\theta^m) + \gamma''(\theta^m)$.

Numerical Results

♠ Model convergence test

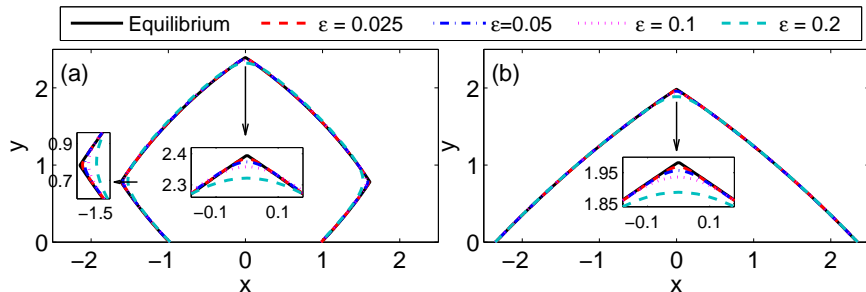
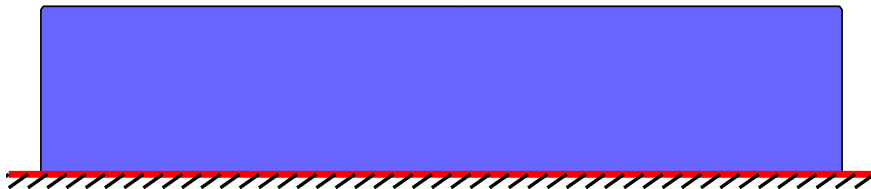


Figure: Comparison of the numerical equilibrium shapes of thin island film with its theoretical equilibrium shape for several values of regularization parameter ε , and the parameters are chosen as (a) $k = 4, \beta = 0.2, \varphi = 0, \sigma = \cos(2\pi/3)$; (b) $k = 4, \beta = 0.2, \varphi = 0, \sigma = \cos(\pi/3)$.

- ♣ Evolution of small thin islands

$$L = 5, m = 4, \beta = 0.2, \sigma = \cos(3\pi/4)$$



- Summary

- PFEM is good to solve the sharp interface model for both weakly and strongly anisotropic surface energies.
- The convergence of the scheme, the effects of the anisotropic on the equilibrium of the thin films and the model convergence for strong case.
- Tends to distribute the mesh points uniformly on the curve according to the arc length automatically.

- Future Work

- Applied the PFEM method to the three dimension sharp interface model.